JACS
JOURNAL OF THE AMERICAN CHEMICAL SOCIETY
Communication
pubs.acs.org/JACS

Boron-Capped Tris(glyoximato) Cobalt Clathrochelate as a Precursor for the Electrodeposition of Nanoparticles Catalyzing H_2 Evolution in Water

Elodie Anxolabéhère-Mallart,[†] Cyrille Costentin,[†] Maxime Fournier,[†] Sophie Nowak,[‡] Marc Robert,[†] and Jean-Michel Savéant*,[†]

[†]Université Paris Diderot, Sorbonne Paris Cité, Laboratoire d'Electrochimie Moléculaire, UMR 7591 CNRS, 15 rue Jean-Antoine de Baïf, F-75205 Paris Cedex 13, France

[‡]Université Paris Diderot, Sorbonne Paris Cité, UFR de Chimie, 15 rue Jean-Antoine de Baïf, F-75205 Paris Cedex 13, France

Supporting Information

ABSTRACT: Electrochemical investigation of a boron-capped tris(glyoximato)cobalt clathrochelate complex in the presence of acid reveals that the catalytic activity toward hydrogen evolution results from an electrodeposition of cobalt-containing nanoparticles on the electrode surface at a modest cathodic potential. The deposited particles act as remarkably active catalysts for H_2 production in water at pH 7.

Platinum is currently used as a catalyst for proton reduction in fuel cells. Replacing this costly metal by cheap, abundant materials is currently an important challenge. Several coordination metal complexes have already been explored for the electrocatalytic hydrogen production, including cobalt,[1] nickel,[2] iron,[3] or molybdenum[4] complexes. Among them, cobalt bisglyoxime complexes are reputed as efficient catalysts,[5] but the mechanism for hydrogen production is still controversial. Mechanisms involving cobalt hydride formation which can evolve through several possible pathways, as recalled in Scheme 1, have been proposed.[5,6] Cobalt chlatrochelate is another family of cobalt catalysts for hydrogen evolution,[7] but the exact catalytic mechanism also remains an open question. Reaction pathways similar to those proposed for cobaloxime complexes can be envisioned.

It is however puzzling that the metal center, buried inside the ligand cavity, could act as an active catalyst. It may accordingly be envisaged that the ligand could play a role as illustrated by pathway ***d*** in Scheme 1. Another possibility is that the actual catalyst would not be the cobalt chlathrochelate itself but a species deriving from its electrochemical transformation. Striking precedence of such processes may be found with oxygen evolving catalysts as, e.g., a manganese cluster complex[8a] as well as a cobalt containing polyoxometalate.[8b] It was shown that the active species are in fact metal oxide nanoparticles rather than the parent homogeneous complexes. Raising the same question of the nature of the actual catalyst, we report the following evidence that the boron-capped tris(glyoximato) cobalt chlathrochelate complex [Co(III)-$(dpg)_3(BF)_2$](BF_4) noted $\mathbf{1}^+$ (BF_4^-) hereafter (Chart 1), with a diphenylglyoxime (dpg) as ligand, reduced in the presence of acid leads to electrodeposition of cobalt containing nanoparticles onto the electrode surface. These nanoparticles are shown to be very active catalysts for H_2 production in water at pH 7.

Scheme 1

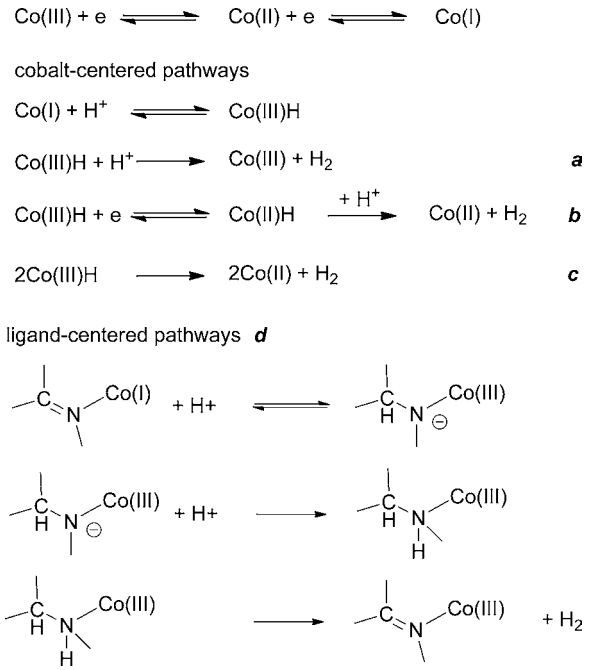

Chart 1. $[Co(dpg)_3(BF)_2]^+$ ($\mathbf{1}^+$)

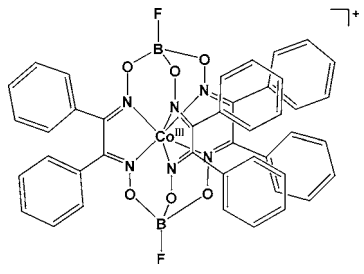

Received: February 3, 2012
Published: March 29, 2012

dx.doi.org/10.1021/ja301134e | J. Am. Chem. Soc. 2012, 134, 6104–6107

In the absence of acid, $\mathbf{1}^+$ gives rise to three cyclic voltammetric reduction waves in acetonitrile (Figure 1a). The

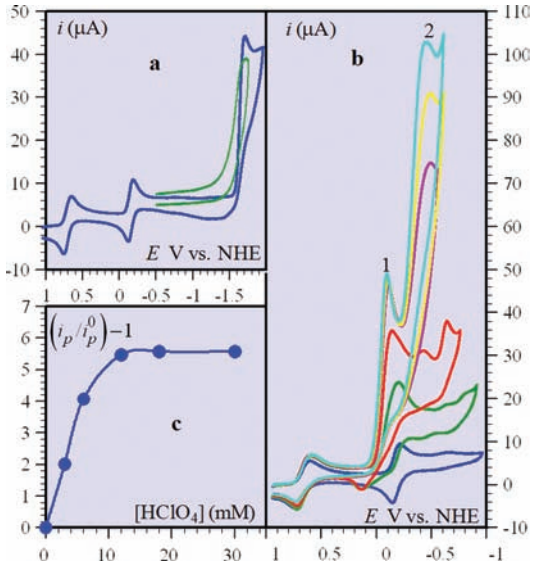

Figure 1. (a, b) Cyclic voltammetry of 0.6 mM $Co[(dpg)_3(BF)_2]BF_4$ with 0.1 M of $NaClO_4$ in acetonitrile. v = 0.1 V/s at a glassy carbon electrode. (a) With no acid present (in green: 0.6 × 3 = 1.8 mM diphenylglyoxime alone); (b) in the presence of increasing concentrations of $HClO_4$ (mM): 0 (blue), 3 (green), 6 (red), 12 (magenta), 18 (yellow), 30 (cyan). (c) Variation of the height of the pseudocatalytic wave 1 with the concentration of acid.

two first reversible waves correspond to the Co^{III}/Co^{II} and Co^{II}/Co^{I} couples successively. The third wave is an irreversible, six-electron wave wave peaking around −1.7 V vs NHE. It corresponds to the reduction of diphenylglyoxime as checked with a solution of the ligand alone three times more concentrated than $\mathbf{1}^+$ (Figure 1b).

Upon addition of perchloric acid, the Co^{II}/Co^{I} wave is strongly enhanced with concomitant loss of reversibility. At first sight, this behavior seems indicative of the occurrence of proton reduction catalysis. Closer examination of the effect of proton and complex concentrations showed that this wave is actually not a catalytic wave. Catalysis of proton reduction in conditions where the acid is in excess over the Co complex should result in an S-shaped wave, the plateau of which should continue to increase with acid concentration, whereas the half-wave potential remains equal to the standard potential of the catalyst.[9] This is not what it is observed (Figure 1b). The wave remains peak-shaped over the whole range of acid concentrations, even when the excess of acid over the complex is as large as 30. The peak height asymptotically reaches an upper limit, which corresponds to the exchange of six electrons per molecule of complex (Figure 1c).[10] The peak potential shifts in the positive direction by as much as 100 mV upon addition of 30 mM $HClO_4$. We may thus conclude that none of the catalytic pathways listed in Scheme 1 is operating.[11] The limiting six-electron stoichiometry points to the hydrogenation of all C−N double bonds of the three diphenylglyoxime ligands, requiring the transfer of two electrons and two protons each. This is exactly the same electron stoichiometry as that for the direct reduction of diphenylglyoxime (green curve in Figure 1a) and the reduction of the diphenylglyoxime ligands in the complex in the absence of acid. The fact that diphenylglyoxime hydrogenation in the presence of $HClO_4$ now takes place at a much more positive potential indicates the occurrence of an intramolecular catalysis of hydrogenation by electrochemically generated Co(I). A detailed analysis of the mechanism of this reaction is beyond the scope of this preliminary communication. However a likely reaction sequence is described in the Supporting Information (SI), which fits the quantitative aspects of the variation of the peak current with concentration of acid and complex as shown in Figure 1c and for other concentrations in the SI. A second peak-shaped wave is observed around −0.45 V vs NHE (noted 2 in Figure 1b), which also grows upon addition of acid. For the same reasons as those for wave 1, this wave does not represent proton reduction catalysis by the complex. Although the stoichiometry could not be investigated in detail as in the case for wave 1, the peak increase is compatible with an overall $12e^- + 12H^+$ stoichiometry, which may likely correspond to the hydrogenolysis of all the N−O bonds ($2e^- + 2H^+$ each) in the boron cap. A more detailed analysis using larger concentrations of acid was precluded by the proximity of a third wave. This wave, noted 3, is shown in Figure 2 (black curve) for a relatively small acid concentration.

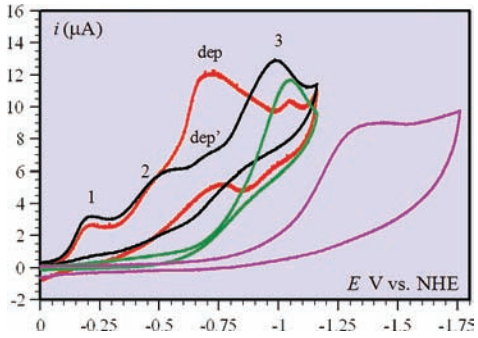

Figure 2. Cyclic voltammograms in acetonitrile + $NaClO_4$ 0.1 M. v = 0.1 V/s at a glassy carbon electrode of 0.1 mM $[Co(dpg)_3(BF)_2]BF_4$ with 3 mM of $HClO_4$. Black: initial scan. Red: after a microelectrolysis at −0.75 V vs NHE during 10 s. Green: 0.1 mM $Co(NO_3)_2$ with 3 mM $HClO_4$. Magenta: 3 mM of $HClO_4$ alone.

This catalytic wave, observed upon a first scan, is located around −1 V vs NHE, whereas direct acid reduction takes place around −1.25 V vs NHE (magenta curve in Figure 2). Wave 3 is similar to the wave observed in a solution of a cobalt salt, $Co(NO_3)_2$, in the presence of the same acid concentration (green curve in Figure 2), thus suggesting a deligation of the metal upon complex reduction. Additional experiments lead to the conclusion that there is in fact a surface modification upon scanning toward cathodic potentials, generating an adsorbed, electroactive new species. After polarizing the electrode at −0.75 V vs NHE for 10 s, a new wave (noted dep in Figure 2) appears around −0.65 V vs NHE of approximately the same height as wave 3. Scanning this new wave makes wave 3 disappear, which is in line with the notion that catalysis at wave dep exhausts the acid in the diffusion-reaction layer.[9c] The initial voltammogram is restored upon careful polishing of the electrode surface.

That electrodeposition on the electrode surface is related to deligation of the complex was confirmed by the disappearance of its UV−vis absorption bands[7a] after electrolysis at −0.75 V vs NHE. An electrolysis at this potential at a glassy carbon foil (see SI) in the conditions depicted in the caption of Figure 3 was then performed. SEM (Scanning Electron microscopy)

dx.doi.org/10.1021/ja301134e | J. Am. Chem. Soc. 2012, 134, 6104−6107

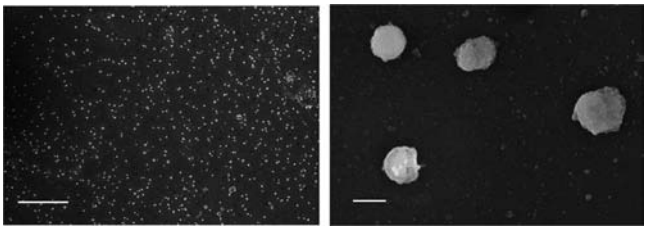

Figure 3. SEM micrographs of nanoparticles deposited on glassy carbon surface (GC foil) after 16 h of electrolysis at −0.75 V vs NHE with 2 mM $Co[(dpg)_3(BF)_2]BF_4$ and 60 mM $HClO_4$ in an acetonitrile solution + 0.1 M $NaClO_4$. Scale bar: 10 μm (left), 300 nm (right).

analysis of the electrode surface after electrolysis shows that nanoparticles (average size 300 nm) have been deposited on the surface (Figure 3). Control SEM images of the carbon surface before electrolysis and after electrolysis at wave 1 (−0.25 V vs NHE), and at wave 2 (−0.55 V vs NHE), showed no particle deposition. Also, no particles were detected on the electrode after electrolysis at −0.75 V vs NHE in a solution containing only $Co(NO_3)_2$ and the acid. The nanoparticles cover a large fraction of the electrode surface, and X-ray diffraction (XRD) as well as energy-dispersive X-ray spectroscopy (EDX) analysis revealed that the particles contain mainly cobalt and oxygen, along with a significant amount of fluorine (see SI). The presence of boron oxide on the carbon surface was also detected. Typical EDX analysis of the nanoparticles gave the following relative atomic average percent (three separate analyses): cobalt = 63 ± 7, oxygen = 22 ± 5, fluorine = 7 ± 1, nitrogen = 3 ± 2 (see SI for details).

Coming back to the experiments summarized in Figure 2, the catalytic response obtained after a microelectrolysis at −0.75 V vs NHE during 10 s (dep wave in red) may therefore be assigned to the deposition of the cobalt nanoparticles on the electrode surface where they catalyze proton reduction. The small dep′ wave on the initial trace in Figure 2 (in black) may be interpreted as resulting from the deposition of a small amount of cobalt nanoparticles during the preceding part of the scan.

Since it is known that electrodeposited cobalt coatings catalyze proton reduction in water,[12] we decided to test the catalytic activity of the nanoparticles deposited in acetonitrile toward H_2 production in water. Electrodeposition on a carbon electrode (either a GC foil for preparative electrolysis or a GC disk electrode for cyclic voltammetry experiments) was then performed at a controlled potential of −0.75 V vs NHE in an acetonitrile solution containing 0.1 mM (respectively 2 mM) of $\mathbf{1}^+$ and 3 mM (respectively 60 mM) of acid during 10 mn (respectively 16 h) when using the disk electrode (respectively the GC foil). After electrolysis, the activated electrode was rinsed and transferred under argon to water containing a phosphate buffer at pH 7 and used as a working electrode for H_2 evolution. At pH 7, the overpotential for proton reduction (defined as the difference between the standard potential of the H^+/H_2 couple at pH 7, −0.42 V vs NHE, and the potential necessary to obtain a given current density) is *ca.* 700 mV at 20 mA/cm^2 (Figure 4). The decrease of the overpotential by reference to a bare electrode is thus 900 mV at this pH (Figure 4) for the same current density.[13]

Preparative scale electrolysis experiments with the activated GC foil as an electrode, poised at −0.75 V vs NHE, led to the results summarized in Figure 5. The catalyst appears to be stable over long electrolysis times. The faradaic yield for H_2 production passes from 75 to 85% during electrolysis, presumably because of the delay between the production of hydrogen bubbles on the surface and the transfer to the headspace over the solution. The cobalt nanoparticles deposited on the surface are thus a very active catalyst, better, concerning cobalt derivatives, than, e.g., the recently reported cobalt pentapyridine complex[1b] and the best of the cobalt dimethylglyoxime complexes reported in ref 14.[15]

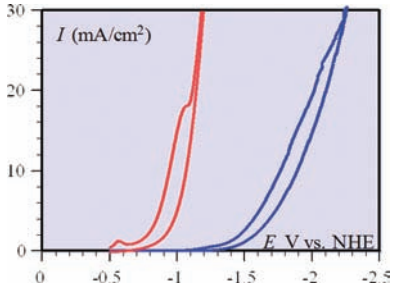

Figure 4. Cyclic voltammograms in water at pH 7 (0.1 M phosphate buffer), at 0.1 V/s, carbon disk electrode. Blue line: bare electrode; red line: electrode activated by deposition of Co nanoparticles (see text).

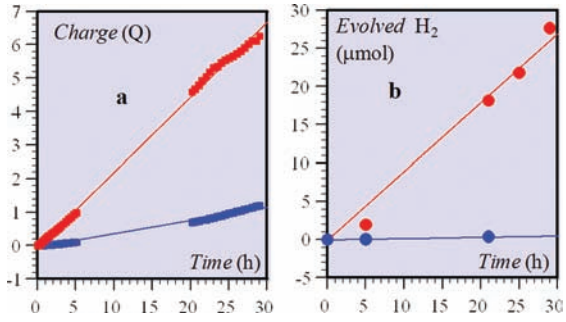

Figure 5. Controlled potential electrolysis (−0.75 V vs NHE) in water at pH 7 in 0.1 M phosphate buffer, at a 1.2 cm^2 double-face GC foil working electrode. (a) Charge vs time. Blue: nonactivated electrode; red: electrode activated by deposition of cobalt containing nanoparticles (see text). (b) H_2 produced (μmol) vs time.

In summary, we have shown that the reduction of an acetonitrile solution of the chlathrochelate cobalt complex $\mathbf{1}^+$, $Co[(dpg)_3(BF)_2]BF_4$ with a diphenylglyoxime (dpg) as ligand, at −0.75 V vs NHE and in the presence of acid leads to the electrodeposition of Co nanoparticles on the electrode surface. These nanoparticles are remarkably active catalysts for H_2 production in water at pH 7 at low overpotential. We have thus unambiguously demonstrated that a non-noble metal complex previously described as a homogeneous catalyst is in fact the precursor of a heterogeneous catalyst. This observation along with recent reports concerning several oxygen-evolving catalysts[8] calls for reevaluation of systems described so far as molecular homogeneous catalysts. Systematic studies of the parameters that govern the electrochemical deposition of active catalytic species seem in order.

■ ASSOCIATED CONTENT

Ⓢ Supporting Information

Experimental details; cyclic voltammetry of $Co[(dmg)_3(BF)_2]$-BF_4; mechanism and cyclic voltammetry simulations for intramolecular catalysis of hydrogenation of the dpg ligands by electrochemically generated Co(I); XRD and EDX analysis of activated surfaces. This material is available free of charge via the Internet at http://pubs.acs.org.

AUTHOR INFORMATION

Corresponding Author

saveant@univ-paris-diderot.fr

Notes

The authors declare no competing financial interest.

ACKNOWLEDGMENTS

Prof. A. Aukauloo is thanked for helpful advice during the synthesis of the complexes, and D. Monteiro for EDX analysis. Partial financial support from the Agence Nationale de la Recherche (ANR 2010 BLAN 0808) is gratefully acknowledged.

REFERENCES

(1) (a) Artero, V.; Chavarot-Kerlidou, M.; Fontecave, M. *Angew. Chem., Int. Ed.* **2011**, *50*, 7238. (b) Sun, Y.; Bigi, J. P.; Piro, N. A.; Tang, M. L.; Long, J. R.; Chang, C. J. *J. Am. Chem. Soc.* **2011**, *133*, 9212. (c) Lee, C. H.; Dogutan, D. K.; McGuire, R.; Nocera, D. G. *J. Am. Chem. Soc.* **2011**, *133*, 8775. (d) Losse, S.; Vos, J. G.; Rau, S. *Coord. Chem. Rev.* **2010**, 2492.

(2) (a) Helm, M. L.; Stewart, M. P.; Bullock, R. M.; Rakowski Dubois, M. R.; Dubois, D. L. *Science* **2011**, *833*, 863. (b) Wilson, A. D.; Shoemaker, R. K.; Miedaner, A.; Muckerman, J. T.; DuBois, D. L.; Rakowski DuBois, M. R. *Proc. Natl. Acad. Sci. U.S.A.* **2007**, *104*, 6951. (c) Rakowski DuBois, M. R.; DuBois, D. L. *Chem. Soc. Rev.* **2009**, *38*, 62.

(3) (a) Bughun, I.; Lexa, D; Savéant, J.-M. *J. Am. Chem. Soc.* **1996**, *118*, 3982. For [Fe]-only and [FeFe] hydrogenase mimics, see: (b) Evans, D. J.; Pickett, C. J. *Chem. Soc. Rev.* **2003**, *32*, 268. (c) Capon, J.-F.; Gloaguen, F.; Schollhammer, P.; Talarmin, J. *Coord. Chem. Rev.* **2005**, *249*, 1664. (d) Tard, C.; Pickett, C. J. *Chem. Rev.* **2009**, *109*, 2245. (e) Gloaguen, F.; Rauchfuss, T. B. *Chem. Soc. Rev.* **2009**, *38*, 100. (f) Singleton, M. L.; Crouthers, D. J.; Duttweiler, R. P.; Reibenspies, J. H.; Darensbourg, M. Y. *Inorg. Chem.* **2011**, *50*, 5015.

(4) (a) Karunadasa, H. L.; Chang, C. J.; Long, J. R. *Nature* **2010**, *464*, 1329. (b) Appel, A. M.; Dubois, D. L.; Rakowski DuBois, M. R. *J. Am. Chem. Soc.* **2005**, 12717.

(5) (a) Connolly, P.; Espenson, J. H. *Inorg. Chem.* **1986**, *25*, 2684. (b) Razavet, M.; Artero, V.; Fontecave, M. *Inorg. Chem.* **2005**, *44*, 4786. (c) Hu, X.; Cossairt, B. M.; Brunschwig, B. S.; Lewis, N. S.; Peters, J. C. *Chem. Commun.* **2005**, 4723. (d) Baffert, C.; Artero, V.; Fontecave, M. *Inorg. Chem.* **2007**, *46*, 1817. (e) Hu, X.; Brunschwig, B. M.; Peters, J. C. *J. Am. Chem. Soc.* **2007**, *129*, 8988. (f) Pantani, O.; Anxolabéhère-Mallart, E.; Aukauloo, A. *Electrochem. Commun.* **2007**, *9*, 54.

(6) (a) Dempsey, J. L.; Brunschwig, B. S.; Winkler, J. R.; Gray, H. B. *Acc. Chem. Res.* **2009**, *42*, 1995. (b) Solis, B. H.; Hammes-Schiffer, S. *Inorg. Chem.* **2011**, *50*, 11252.

(7) (a) Pantani, O.; Naskar, S.; Guillot, R.; Millet, P.; Anxolabéhère-Mallart, E.; Aukauloo, A. *Angew. Chem., Int. Ed.* **2008**, *120*, 9948. (b) Millet, P.; Mbemba, N.; Grigoriev, S. A.; Fateev, V. N.; Aukauloo, A.; Etiévant, C. *Int. J. Hydrogen Energy* **2011**, *36*, 4134. (c) Voloshin, Y. Z.; Dolganov, A. V.; Varzatskii, O. A.; Bubnov, Y. N. *Chem. Commun.* **2011**, *47*, 7737.

(8) (a) Hocking, R. K.; Brimblecombe, R.; Chang, L. Y.; Singh, A.; Cheah, M. H.; Glover, C.; Casey, W. H.; Spiccia, L. *Nat. Chem.* **2011**, *3*, 461. (b) Stracke, J. J.; Finke, R. G. *J. Am. Chem. Soc.* **2011**, *133*, 14872.

(9) (a) Savéant, J.-M.; Vianello, E. In *Advances in Polarography*; Longmuir, I. S., Ed.; Pergamon Press: London, 1960; pp 367−374. (b) Savéant, J.-M.; Su, K. B. *J. Electroanal. Chem.* **1984**, *171*, 341. (c) Savéant, J.-M. *Elements of Molecular and Biomolecular Electrochemistry*; Wiley-Interscience: New York, 2006; Chap. 2, pp 108−119. (d) Savéant, J.-M. *Chem. Rev.* **2008**, *108*, 2348.

(10) (a) The same observation was made with toluenesulfonic acid (pK = 8) and trifluoroacetic acid (pK = 12.7) as compared to $HClO_4$ (pK = 2).[10b] (b) Izutsu, K. *Acid-base dissociation constants in dipolar aprotic solvents*; Blackwell: Boston, 1990; pp 17−35.

(11) A similar behavior is observed with a similar complex, $Co[(dmg)_3(BF)_2]BF_4$, in which the phenyl groups of the $Co[(dpg)_3(BF)_2]BF_4$ complex have been replaced by methyl groups (see SI).

(12) Soto, A. B.; Arce, E. M.; Palomar-Pardavé, M.; Gonzalez, I. *Electrochim. Acta* **1996**, *41*, 2647.

(13) We observed from experiments made at pH 6, 7, and 8 that the overpotential remains constant at given current density, implying a proton reaction order of 1.

(14) McCrory, C. C. L.; Uyeda, C.; Peters, J. C. *J. Am. Chem. Soc.* **2012**, *134*, 3164.

(15) (a) 59 mV-extrapolation of the electrolysis current densities at zero overpotentials leads to log $I_{\eta=0}$ (mA/cm^2) = −7.3 as compared to −14.7 for ref 1b and −10.5 for ref 14. Better efficiencies are obtained with derivatives of other metals.[15b,c] (b) Le Goff, A.; Artero, V.; Jousselme, B.; Tran, P. D.; Guillet, N.; Métayé, R.; Fihri, A.; Palacin, S.; Fontecave, M. *Science* **2009**, *326*, 1384. (c) Merki, D.; Fierro, S.; Vrubel, H.; Hu, X. *Chem. Sci.* **2011**, *2*, 1262.